

---

# The trade off issues reduction for PAPR by using Hadmard technique in OFDM

---

S.Mabu Subhani & Sk.Md.Shareef

P.G. Scholar, Eswar College Of Engineering, Narasropet, Guntur Dt.

Mail Id:Subhanimabu789@Gmail.Com

Asst.Professor, Dept Of E.C.E, Eswar College Of Engineering, Narasaraopet, Guntur Dt.

Mail Id:Shareef490@Gmail.Com

## Abstract:

*To lessen the PAPR in OFDM frameworks chose mapping plans (SLM) are broadly utilized due its twisting less nature. However a noteworthy downside of conventional SLM system is high computational many-sided quality to choose a low PAPR flag it requires a bank of reverse quick Fourier (IFFT) operations. This paper proposes a novel engineering for PAPR decrease in OFDMs with low computational many-sided quality. In this proposed technique, recurrence space cyclic moving, complex conjugate, sub-bearer inversion operations are performed to build the PAPR diminishment execution in OFDM frameworks though in customary SLM conspire just recurrence area stage turn can be performed to create the competitor signals. Moreover, to diminish the various IFFT issues, the greater part of the recurrence area equal operations are changed over into time-space counterparts. It is demonstrated that the sub bearer parceling and re-gathering forms are vital in acknowledging low multifaceted nature time space proportionate operations. In addition, it is indicated hypothetically and numerically that the computational multifaceted nature of the proposed conspire is fundamentally lower than the conventional SLM strategy and the PAPR lessening execution is inside 0.001 dB of that SLM. Watchwords: Orthogonal Frequency Division Multiplexing (OFDM), Peak to Average Power Ratio(PAPR), Selected Mapping Scheme (SLM).*

## I.Introduction

After over thirty years of innovative work, OFDM has been widely adjusted in remote correspondences because of its low weakness to multipath engendering and high ghostly proficiency. In numerous applications, high information rate transmissions are required over remote channels with OFDM frameworks. However a noteworthy disadvantage of OFDM based transmission framework is its high PAPR, which prompts in-band bending and out of band radiation when the signs are gone through a non-direct power speaker. There are different proposition for PAPR lessening in OFDM frameworks in writing, including tone reservation, tone infusion, cutting, halfway transmit succession, active constellation augmentation, nonlinear companding, chose mapping(SLM). Among every one of these systems SLM is most ordinarily utilized because of its mutilation less nature. However a noteworthy disadvantage of conventional SLM method is high computational

unpredictability to choose a low PAPR flag it requires a bank of backwards quick Fourier (IFFT) operations. To decrease the computational multifaceted nature, a few low-unpredictability SLM designs have been proposed [14]-[16] in which the recurrence area stage pivots are changed over into comparable recurrence space stage turns. This paper proposes a novel design for PAPR

lessening in OFDMs with low computational many-sided quality. In this proposed technique, recurrence area cyclic moving, complex conjugate, sub-bearer inversion operations are performed to build the PAPR assorted variety in OFDM frameworks while in conventional SLM plot just recurrence space stage turn is utilized to create the applicant signals. II. MODEL OF A SYSTEM Consider an OFDM framework with N-subcarriers. Give the balanced images a chance to frame a  $N \times 1$  recurrence area information vectors is given by,

$$X = [X[0], X[1], \dots, X[N - 1]]^T,$$

where  $X[K]$  denotes the modulated symbol of the Kth sub-carrier and  $(\cdot)^T$  is transpose operation. An N-point operation of time domain signal vector of  $x$  is given by

$$x[n] = \frac{1}{\sqrt{N}} \sum_{k=0}^{N-1} X[k] \cdot \exp\left\{j\frac{2\pi nk}{N}\right\}, \quad (1)$$

$$n = 0, 1, 2, \dots, N - 1$$

The PAPR of the discrete time OFDM signal is given by,

$$PAPR(X) = \frac{\max_{0 \leq n \leq N-1} |x[n]|^2}{E[|x[n]|^2]} \quad (2)$$

Where  $E[\cdot]$  denotes expectation operation. For OFDM systems generally complementary cumulative distribution function is used to evaluate the PAPR reduction performance. The CCDF is used to measure the probability that the PAPR of a certain data block exceeds the given threshold  $\gamma$  i.e. ,

$$CCDF_{PAPR(X)} = Pr(PAPR(X) > \gamma) \quad (3)$$

### III. PAPR REDUCTION OF OFDM SYSTEMS IN FREQUENCY DOMAIN

This section describes the implementation of PAPR reduction in OFDM systems in frequency domain. In this conspire, the PAPR assorted variety of the competitor signals is expanded by performing recurrence area cyclic move complex conjugate, subcarrier inversion operations while in conventional SLM plot, the hopeful signs are produced by performing recurrence space stage turn as it were. Consider an OFDM framework with N subcarriers. Let the N subcarriers are parceled into S subcarriers sets  $\Gamma_s, s=0, 1, \dots, S-1$ . For the most part, there are three strategy for parceling the subcarriers in OFDM frameworks in particular, limited dividing technique (LPM), circulated apportioning technique (DPM), cross breed parceling technique (HPM). In LPM each sub-transporter set comprises of various contiguous and continuous sub bearers. In the mean time, in DPM each sub bearer set comprises of a different interleaved subcarriers with rise to separating. At long last in HPM the subcarriers are first apportioned into U confined subcarriers sets and those subcarriers are additionally divided into V appropriated subcarrier sets. It ought to be noticed that all the recurrence space operations depicted in the accompanying are performed at the subcarrier set level i.e.,  $X_s$ . Fig. 1 shows a piece chart of the proposed PAPR lessening plan in the recurrence space, where the recurrence area information vector  $X$  is apportioned into S  $N \times 1$  information vectors  $X_s, s = 0, 1, \dots, S - 1$ . It is noticed that keeping in mind the end goal to permit the greatest adaptability in dividing the sub-transporter, the sub-bearers are parceled utilizing the HPM strategy. As appeared in Fig.1, the S information vectors  $X_s, s=0, 1, \dots, S-1$  are handled by numerous applicant flag producing pieces (CSGBs) so as to create the hopeful signs.

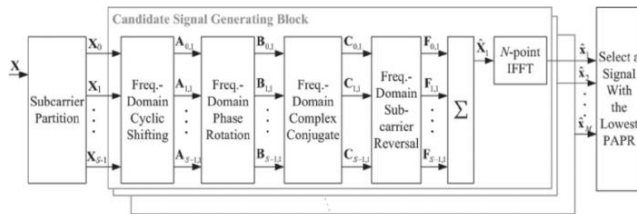


**Fig. 1. System architecture of proposed scheme in frequency domain.**

(Note that each CSGB generates a single candidate signal.) For illustration purposes, consider the *m*th CSGB in Fig.1. The first block in the CSGB performs a frequency-domain cyclic shifting operation. Assuming that  $l_{s,m}$  cyclic shifts are performed on  $X_s$ , the output signal is denoted as  $A_{s,m}$ ,  $s=0,1,\dots,S-1, m=1,2,\dots,M-1$ .

Therefore, the *k*th element of  $A_{s,m}$  is given by

$$A_{s,m}[k] = X_s \left[ (k - l_{s,m})_N \right] \tag{4}$$

$$k = 0, 1, \dots, N - 1$$

Where  $(\cdot)_N$  denotes the modulo *N* operation. Note that the selection of the cyclic shift value  $l_{s,m}$  for a given *m* is not arbitrary, but is jointly considered over various *s* since different sub-carrier sets cannot occupy the same sub-carrier after the cyclic shifting operation. The second block of the CSGB performs phase rotation in frequency domain. The output of the *S*th subcarrier set for the *m*th CSGB is denoted as  $B_{s,m}$ , with the *k*th element is given by

$$B_{s,m}[k] = \theta_{s,m}[k] \cdot A_{s,m}[k] \tag{5}$$

$$k = 0, 1, \dots, N - 1,$$

where  $\theta_{s,m}[k]$  is a complex number with a unit magnitude.

The third block of the CSGB performs a frequency-domain conjugate operation and the output signal is denoted by  $C_{s,m}$ . Each

subcarrier set chooses arbitrarily whether to perform or not to perform the conjugate operation, in order to generate candidate signals with an uncorrelated PAPR.

$$C_{s,m}[k] = B_{s,m}[k] \text{ or } C_{s,m}[k] = B_{s,m}^*[k], \forall k \in \Gamma_s \tag{6}$$

where  $*$  denotes the complex conjugate operation. The fourth block of the CSGB performs a sub-carrier reversal operation in frequency domain on the sub-carrier sets, i.e., the output signal is given by

$$F_{s,m}[k] = C_{s,m}[(-k)_N], \forall k \in \Gamma_s \tag{7}$$

The choice of whether or not to perform the reversal operation is not arbitrary, but is jointly considered since different subcarrier sets cannot occupy the same sub-carriers after the subcarrier reversal process. Notably, as for the conjugate operation, each sub-carrier set may or may not choose to perform sub-carrier reversal. Finally, the *m*th candidate signal in the frequency domain is obtained by summing up the sub-carrier sets of the corresponding CSGB, i.e.,

$$\hat{X}_m = \sum_{s=0}^{S-1} F_{s,m} \tag{8}$$

The hopeful flag in the time space, i.e.,  $X_m$  is gotten by playing out an IFFT operation on  $\hat{X}_m$ . Among all the produced hopeful flags, the flag with least PAPR is chosen for transmission. The above plan requires MIFFT operations. Subsequently, the computational many-sided quality of the proposed conspire is greatly high. Hypothetically, this issue can be kept away from by changing over each of the four recurrence space operations into time-area counterparts. Be that as it may, by basically considering the comparing IFFT, the transformation procedure can't be performed since the time-area operations ought to

likewise have a low computational intricacy. In this way, in the accompanying area, an all the more computationally-productive approach is proposed.

#### IV. TIME DOMAIN EQUIVALENT PROPERTIES OF OFDM SYSTEMS

In this area, to decrease the computational many-sided quality of the recurrence space engineering each of the four recurrence space operations are changed over into identical time space operations. What's more, a period space redundancy property is acquainted all together with additionally decrease the computational many-sided quality. Note that all of the operations described in this section (both frequency-domain and time domain) are performed on the sub-carriers of the same set.

**Property1: Frequency-Domain Cyclic Shifting/Time Domain Phase Rotation**  
Performing cyclic shifting on the frequency-domain data vector  $X$  is equivalent to performing phase rotation on the corresponding time-domain data vector  $x$ , i.e.,

$$F^{-1}\{X[(k-l)_N]\} = x[n] \cdot \exp\left\{\frac{j2\pi nl}{N}\right\} \quad (9)$$

Where  $F^{-1}[\cdot]$  denotes the IFFT operation, and  $l$  is the number of frequency-domain cyclic shifts. Note that for  $l \in$

$$\left\{0, \frac{N}{4}, \frac{N}{2}, \frac{3N}{4}\right\}, \text{ we have } \exp\left\{\frac{2\pi jnl}{N}\right\} \in \{\pm 1, \pm j\} \text{ and the time-}$$

domain equivalent operation on the right hand side of (8) does not require any complex multiplications or additions Note also that the choice of cyclic shifts  $l$  is not arbitrary.

**Property 2: Frequency-Domain Phase Rotation / Time-Domain Cyclic Shifting**  
Performing phase rotation on the frequency-domain data vector  $X$  is equivalent to

performing cyclic shifting on the corresponding time-domain data vector  $x$ , i.e

$$F^{-1}\left\{X[k] \cdot \exp\left\{\frac{-j2\pi k\omega}{N}\right\}\right\} = x[(n-\omega)_N], \quad (10)$$

$$\omega = 0, 1, \dots, N-1$$

**Property3: Frequency-Domain Complex Conjugate Time-Domain Complex Conjugate of Time-Reversed Signals**  
Performing the frequency-domain complex conjugate operation is equivalent to performing the complex conjugate operation on the time-reversed signals, i.e.,

$$F^{-1}\{X^*[k]\} = x^*[(-n)_N] \quad (11)$$

**Property4: Frequency-Domain Sub-carrier Reversal/Time -Domain Signal Reversal**  
Performing sub-carrier reversal on the frequency-domain data vector  $X$  is equivalent to performing time-domain reversal operation on data vector  $x$ , i.e.,

$$F^{-1}\{X[(-k)_N]\} = x[(-n)_N] \quad (12)$$

It ought to be noticed that the recurrence area sub-bearer inversion operation can't be performed on self-assertive sub-transporter sets since this may bring about various sub-bearer sets possessing a similar sub-bearers. In this manner, various comments are given in the accompanying to elucidate the materialness of the subcarrier inversion operation for the three sub-bearer dividing strategies. Property 5: Time-Domain Repetition In DPM, the recurrence area sub-bearers of any set  $\Gamma$  have an equivalent separating  $S$ . Therefore, the time-space flag vector  $X_s$  has the accompanying redundancy trademark:

$$X_s = [X_s^{(0)} \quad \beta_{s,1} X_s^{(0)} \quad \beta_{s,2} X_s^{(0)} \quad \dots \quad \beta_{s,S-1} X_s^{(0)}]^T \quad (13)$$

where  $x(0)$  is a  $1 \times \frac{N}{S}$  vector consisting of the first  $\frac{N}{S}$  elements of  $X_s, \beta_{s,i} = \exp\{j2\pi i \cdot \frac{s}{S}\}, i = 1, 2, \dots, S - 1$ . It is noted that  $\beta_{s,i} \in \{\pm 1, \pm j\}, S = 2, 4$ .

Furthermore, in HPM, the sub-carriers have an equal spacing of  $V$ . Thus, the following property can be obtained:

$$X_s = [X_s^{(0)} \quad \beta_{s,1}X_s^{(0)} \quad \beta_{s,2}X_s^{(0)} \quad \dots \quad \beta_{s,V-1}X_s^{(0)}]^T \quad (14)$$

Where  $X_s^{(0)}$  is a  $1 \times \frac{N}{S}$  vector consisting of first  $\frac{N}{S}$  elements of  $X_s$ ,  $\beta_{s,i} = \exp\{j2\pi i \cdot \frac{s}{V}\}, i' = 1, 2, \dots, V - 1, \beta_{s,i'} \in \{\pm 1, \pm j\}$ .

## V. PROPOSED PAPR REDUCTION OF OFDM SYSTEMS IN TIME DOMAIN

The above Section has portrayed the execution of the proposed PAPR lessening plan in the recurrence area. In any case, as talked about, for every age of an applicant flag it requires a  $N$ -point IFFT operation. In the event that the age of hopeful signs expands the quantity of  $N$ -point operations increments and it comes about as a high computational intricacy plot. To determine the issue of high computational many-sided quality, this segment uses the time-space proportional operations to develop a low-multifaceted nature design for PAPR diminishment. Fig.2 presents a piece outline of the proposed engineering, in which the recurrence area information vector  $X$  is apportioned into  $S$  information vectors  $X_s$  of size  $N \times 1, s = 0, 1, \dots, S-1$ . Note that in actualizing the proposed engineering, the HPM sub-transporter dividing strategy is received keeping in mind the end goal to expand the PAPR decent variety. As appeared in Fig. 2, having divided the sub-bearers, an IFFT operation is performed  $X_s$  on to get the relating time-space information vector  $X_s$  of size  $N \times 1$ . It is noticed that in spite of the fact that the proposed conspire still requires  $S$   $N$ -point IFFT operations, the computational many-sided quality of the proposed

engineering is much lower than that of the customary SLM plot since  $S$  is substantially littler than the quantity of competitor signals  $M$ . Besides, the computational many-sided quality of every  $N$ -point IFFT is essentially diminished in the proposed plot since the greater part of the components of  $X_s$  are zero. Following the IFFT operations, the time-space information vectors  $X_s, s = 0, 1, \dots, S - 1$ , are prepared by  $M$  CSGBs with a specific end goal to create  $M$  hopeful signs. It is noticed that the summation of  $X_s$  produces the first run through area transmitted flag. In each of the  $M$  CSGBs, each  $X_s$  is first handled when space stage revolution piece (i.e., the time-area likeness the recurrence area cyclic moving operation). The subsequent yield flag is indicated  $a_{s,m}$ , where the  $n$ th component is given by

$$a_{s,m}[n] = X_s[n] \cdot \exp\left\{\frac{j2\pi n \cdot l_{s,m}}{N}\right\}, \quad (15)$$

$$n = 0, 1, \dots, N - 1$$

in which  $X_s[n]$  is the  $n$ th element of  $X_s$  and  $l_{s,m}$  is the number of frequency-domain cyclic shifts of  $\Gamma_s$  for the  $m$ th candidate signal. The second block of the CSGB performs a time domain cyclic shifting operation, i.e., the time-domain equivalent of the frequency-domain phase rotation operation. Therefore, the  $n$ th element of the output signal  $b_s$ , has the form of

$$b_{s,m}[n] = a_s \left[ (n - \omega_{s,m})_N \right] \quad (16)$$

$$n = 0, 1, \dots, N - 1$$

Where  $\omega_s$ , denotes the number of cyclic shifts of the  $s$ th sub-carrier set for the  $m$ th CSGB. It will be reviewed that the recurrence area stage pivot operation isn't self-assertive. By and by, stage revolution isn't totally irregular, and along these lines the PAPR

decrease execution is marginally debased. In any case, this downside is minor contrasted with the generous decrease accomplished in the computational many-sided quality of the proposed conspire. The third piece in Fig.2 plays out the time-space complex conjugate operation, i.e., the proportional operation of the recurrence area complex conjugate process. Since the framework subjectively picks regardless of whether to play out the mind boggling conjugate operation, the  $n$ th component of the yield flag  $C_s$ , has the shape

$$c_{s,m}[n] = b_{s,m}[n] \quad \text{or} \quad b_{s,m}^*[(-n)_N]$$

As discussed in Section III (Property 4), the sub-carrier sets must be properly re-assembled before performing the time domain signal reversal operation. In particular, when using the HPM partitioning method, the sub-carrier sets must be reassembled in such a way that the partition is equivalent to that obtained using DPM (Remark 3).

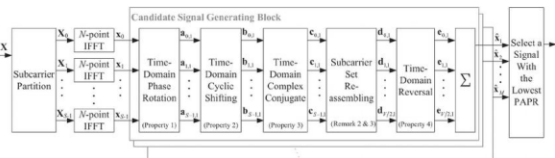


**Fig. 2. System architecture of proposed scheme in time domain.** Furthermore, for the case of DPM, the time-domain signal reversal operation can be applied on either  $\Gamma s=0$  or  $\Gamma s=S/2$  individually, but should be performed on  $\Gamma s$  and  $\Gamma s-S$  simultaneously,  $s=1,2,\dots,S/2-1$  in order to avoid sub-carrier overlaps (Remark 2). Therefore, the fourth block of the time-domain CSGB performs a subcarrier set re-assembling function, which consists of the two steps. In the first step, the  $S$  HPM sub-carrier sets  $\Gamma s$ ,  $s=0,1,\dots,S-1$  ( $S=U.V$ ), are combined to obtain the  $V$  DPM subcarrier sets  $\Gamma s$ ,  $s=0,1,\dots,V-1$ . The  $s$ th DPM sub-carrier set is obtained by combining the outputs of time-

domain complex conjugate operations  $c_{u.v+s,m}$ ,  $u=0,1,\dots,U-1$  i.e.,

$$\bar{c}_{\bar{s},m} = \sum_{u=0}^{U-1} c_{(u.v+\bar{s}),m}, \quad \bar{s} = 0,1,\dots,V-1 \quad (18)$$

In the second step, sub-carrier sets are  $\Gamma s$  and  $\Gamma S-s$ ,  $s=0,1,\dots,V/2-1$  are combined to form a single sub carrier set  $\Gamma q$ ,  $q=0,1,2,\dots,V/2-1$ , while leaving  $\Gamma s=0$  and  $\Gamma s=V/2$  unchanged i.e.,

$$d_{q,m} = \begin{cases} c_{0,m}, & q = 0, \\ \bar{c}_{\frac{V}{2},m}, & q = \frac{V}{2}, \\ \bar{c}_{q,m} + \bar{c}_{V-q,m}, & q = 1,2,\dots,\frac{V}{2}-1. \end{cases} \quad (19)$$

Substituting (18) into (19) yields,

$$d_{q,m} = \begin{cases} \sum_{u=0}^{U-1} c_{u.v,m}, & q = 0, \\ \sum_{u=0}^{U-1} c_{u.v+\frac{V}{2},m}, & q = \frac{V}{2}, \\ \sum_{u=0}^{U-1} c_{u.v+q,m} + \sum_{u=0}^{U-1} c_{u.v+(V-q),m}, & q = 1,2,\dots,\frac{V}{2}-1 \end{cases} \quad (20)$$

is significant that all operations previously re-massing are performed by HPM. Along these lines, the subsequent signs are not comparable to those gotten by DPM from the earliest starting point. It is noticed that the Sub-transporter Set Re-assembling piece of the proposed time-space engineering utilizes the time-area redundancy property (i.e., Property 5) with a specific end goal to diminish the computational intricacy. The sub-transporter set re-collecting operation is trailed when space flag inversion process (see Fig.2). Similarly as with the mind boggling conjugate operation, the framework self-assertively picks regardless of whether to play out the inversion operation. The  $n$ th component of the subsequent flag  $e_{q,m}$ ,  $q=0,1,\dots,V/2$ , therefore has the form

$$e_{q,m}[n] = d_{q,m}[n] \quad \text{or} \quad d_{q,m}^*[(-n)_N], \quad q = 0,1,\dots,\frac{V}{2} \quad (20)$$

Finally, the  $m$ th candidate signal is obtained by adding all the  $e_{q,n}$  of the  $m$ th CSGB, to give

$$x_m = \sum_{q=0}^{V/2} e_{q,m} \quad (21)$$

Having produced  $M$  competitor flags, the flag with the most minimal PAPR is chosen for transmission. It ought to be noticed that the proposed scheme requires different operations at the transmitter, however the related parameters can be put away at both the transmitter and recipient with code book. Along these lines, the quantity of side data bits depends just on the quantity of hopeful signs. On the off chance that  $M$  competitor signals are created, the plan requires just  $\log_2 M$  bits to transmit side data. Moreover, the side data is thought to be transmitted through the control channel, where channel coding is received to shield the side data from being wrongly recognized.

## VI. ANALYSIS OF COMPUTATIONAL COMPLEXITY

This section evaluates the computational complexities of the traditional SLM scheme and the proposed PAPR reduction scheme, respectively. The traditional SLM scheme requires  $M$   $N$ -point IFFTs to generate  $M$  different candidate signals, where each  $N$ -point IFFT requires  $N^2 \cdot \log_2 N$  complex multiplications and  $N \cdot \log_2 N$  complex additions. Therefore, the total number of complex multiplications and complex additions are  $MN^2 \cdot \log_2 MN$  and  $MN \cdot \log_2 N$ , respectively. For the PAPR reduction scheme proposed in this study, a total of  $S$   $N$ -point IFFTs and  $M$  CSGBs are required to generate  $M$  candidate signals. The HPM partitioning method is adopted in order to maximize the PAPR diversity. Therefore, the sub-carriers are partitioned into  $S = U \cdot V$  sets. In the proposed architecture, most

elements of the inputs to the IFFTs, i.e.,  $X_s$  in (4), are zeros, and thus the IFFTs can be readily computed using the efficient algorithm proposed in [19]. It can be shown that the total number of complex multiplications and complex additions for  $S$  IFFT operations is therefore equal to  $UN^2 \cdot \log_2 NUV + N \cdot U - 1$  and  $UN \cdot \log_2 UN$  respectively. Regarding the computational complexity of each CSGB, Property 1 demonstrates that the time-domain equivalent operation on the right hand side of (8) does not require any complex multiplications or additions when the number of frequency-domain cyclic shifts belongs to  $0, N/4, N/2, 3N/4$  which implies that  $U = 2$  or  $U = 4$  should be adopted. Furthermore, Property 5 indicates that  $V = 2, 4$  yields a significant reduction in the computational complexity. Therefore, four different combinations of  $U$  and  $V$  are considered in the remainder of this study, i.e.,  $U, V = \{2, 2, 2, 4, 4, 2, (4, 4)\}$ . However, increasing  $U$  and  $V$  increases the complexity of the PAPR reduction process. Furthermore, a series of preliminary simulations showed that there was no significant change in the PAPR reduction performance of the proposed scheme when using higher values of  $U$  and  $V$  as shown in Fig.3. Thus, in evaluating the performance of the proposed scheme, higher values of  $U$  and  $V$  were not considered. Since  $U = 2, 4$  and  $V = 2, 4$  were adopted, the first three blocks of the CSGBs in the proposed scheme, i.e., the time-domain phase rotation, time-domain cyclic shifting, and time-domain complex conjugate operations, do not require any complex multiplications or additions, as indicated in Property 1, 2, and 3.

SLM strategy and the technique proposed by Li and Wang [15] for correlation purposes. It is seen that the number of complex augmentations in the customary SLM plot

increments with an expanding number of competitor signals. In any case, in the proposed conspire and that of Li furthermore, Wang, the quantity of complex augmentations stays steady, regardless of the quantity of applicant motions as appeared in Fig.4. Of the three plans, the technique proposed in [15] requires minimal number of complex duplications, trailed by the plan proposed in this examination with  $(U, V) = (2, 4)$  and  $(U, V) = (2, 2)$ . By differentiate, the proposed conspire with  $(U, V) = (2, 2)$  requires the insignificant number of complex increments, taken after by Li and Wang's strategy and the proposed plot with  $(U, V) = (2, 4)$ .

### VII. SIMULATION RESULTS

The PAPR reduction performance of the proposed scheme was evaluated by means of numerical simulations. Fig5 shows the PAPR reduction performance of the proposed scheme for an OFDM system with 256 sub-carriers and the 16-quadrature amplitude modulation (16- QAM) scheme. It can be seen that the PAPR reduction performance of the proposed scheme with  $(U, V) = (4, 4)$  is extremely close to that of the traditional SLM method.

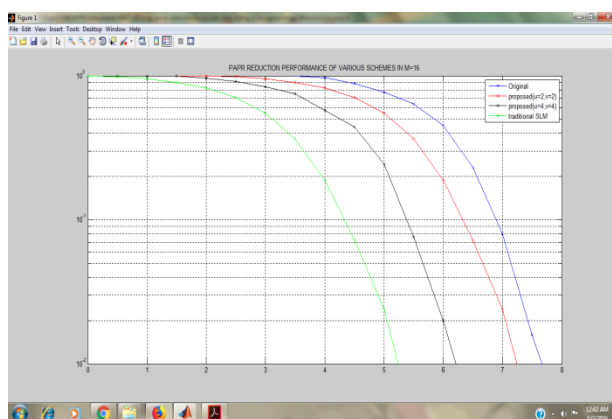


FIG 3: PAPR REDUCTION PERFORMANCE OF VARIOUS SCHEMES IN M=16

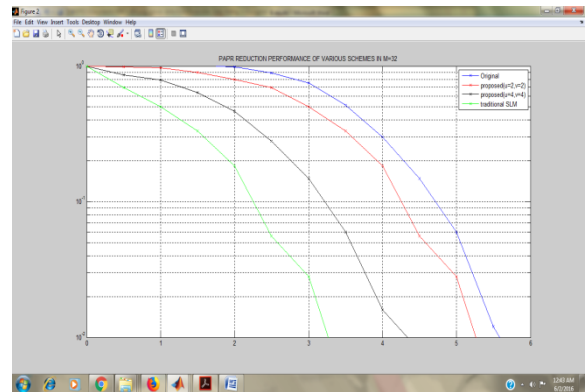


FIG 4: PAPR REDUCTION PERFORMANCE OF VARIOUS SCHEMES IN M=32

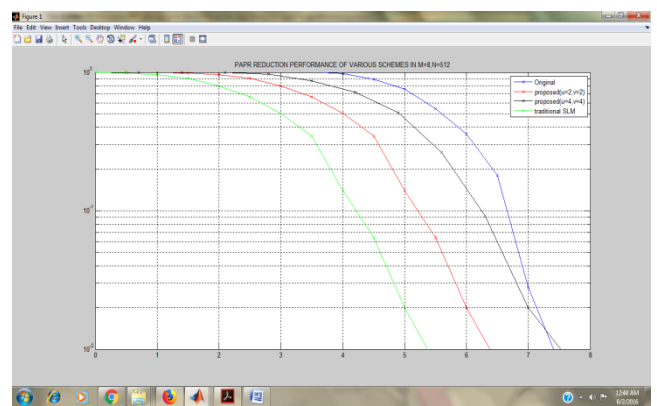


FIG 5: PAPR REDUCTION PERFORMANCE OF VARIOUS SCHEMES IN M=8, N=1024

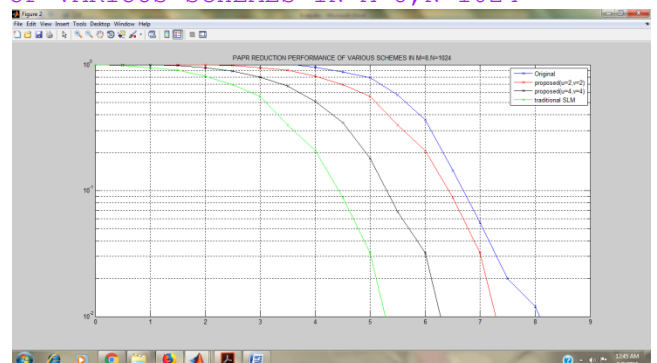


FIG 6: PAPR REDUCTION PERFORMANCE OF VARIOUS SCHEMES IN M=8, N=512

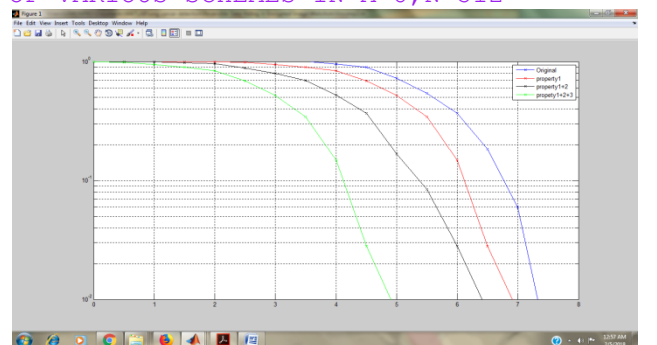


FIG: PAPR reduction performance of various combinations of frequency domain



operations (16-QAM,  $M = 32$ ,  $N = 256$ ,  $U = 4$ ,  $V = 4$ ).

From a detailed inspection, the performance loss of the proposed scheme relative to that of the traditional SLM method is found to be less than 0.001 dB for  $M = 32$ ,  $U = 4$ ,  $V = 4$ , and  $Pr(PAPR X > \gamma = 10^{-4})$ . Fig. 6 demonstrates the PAPR reduction performance for the cases of  $N = 512$  and  $N = 1024$ . It can be seen that PAPR increases with the number of sub-carriers. However, the PAPR reduction performances of the proposed scheme are able to approach those of the traditional SLM scheme. A series of simulation experiments are conducted to investigate the PAPR reduction performance when various combinations of frequency-domain operations are performed. The results are demonstrated in Fig7, where the PAPR reduction performance basically increases with the number of extra frequency-domain operations. Fig.7 indicates that the improvement for Properties 1+2+3 is only marginal compared with Properties 1+2. Thus, the contribution of Property 3 (frequency-domain complex conjugate) is insignificant. However, the PAPR reduction performance when Properties 1+3 are adopted is better than when Property 1 alone is adopted. Therefore, the effect of equivalent frequency-domain operation in PAPR reduction depends on their order of operations. In addition, the PAPR reduction performance in general increases with the number of frequency-domain operations.

## IX. CONCLUSION

Contrasted with the customary SLM plot, in which the competitor signals are created utilizing frequencydomain stage turn just, a novel engineering is proposed in this examination which furthermore utilizes three operations to be specific, recurrence space

cyclic moving, complex conjugate and sub-transporter inversion operations can be performed to amplify the PAPR decrease execution of the competitor signals. To maintain a strategic distance from the numerous IFFT issue characteristic in the customary SLM strategy, the proposed conspire changes over every one of the four recurrence space operations into time-area proportional operations. It has been demonstrated that the computational multifaceted nature of the proposed approach can be limited through a proper parceling and reassembling of the sub-bearers in the OFDM framework. What's more, the hypothetical examination comes about have demonstrated that the quantity of complex duplications and complex increases required in the proposed conspire for  $(U, V) = (4, 4)$  are 8.59% and 68.75%, separately, of those required in the conventional SLM conspire. Moreover, the recreation comes about have demonstrated that the execution loss of the proposed plot in respect to that of the customary SLM plot is not exactly 0.001 dB for 16-QAM,  $M = 32$ ,  $N = 256$ ,  $U = 4$ ,  $V = 4$ , and  $Pr PAPR X > \gamma = 10^{-4}$ . As it were, the proposed plot nearly approximates the PAPR lessening execution of the customary SLM technique, however with an altogether diminished computational many-sided quality.

## X. REFERENCES

- [1]J.-C. Chen and C.-P. Li, "Tone reservation using near-optimal peak reduction tone set selection algorithm for PAPR reduction in OFDM systems," IEEE Signal Process. Lett., vol. 17, no. 11, pp. 933–936, Nov.2010.
- [2]H. Li, T. Jiang, and Y. Zhou, "An improved tone reservation scheme with fast convergence for PAPR reduction in OFDM systems," IEEE Trans Broadcast., vol. 57, no. 4, pp. 902–906, Dec. 2011.

- [3]S. Gazor and R. AliHemmati, "Tone reservation for OFDM systems by maximizing signal-to-distortion ratio," *IEEE Trans. Wireless Commun.*, vol. 11, no. 2, pp. 762–770, Feb. 2012.
- [4]T. Jiang, W. Xiang, P. C. Richardson, D. Qu, and G. Zhu, "On the nonlinear companding transform for reduction in PAPR of MCM signals," *IEEE Trans. Wireless Commun.*, vol. 6, no. 6, pp. 2017–2021, Jun. 2007.
- [5]J.-C. Chen and C.-K. Wen, "PAPR reduction of OFDM signals using cross-entropy-based tone injection schemes," *IEEE Signal Process. Lett.*, vol. 17, no. 8, pp. 727–730, Aug. 2010.
- [6]B. S. Krongold and D. L. Jones, "PAR reduction in OFDM via active constellation extension," *IEEE Trans. Broadcast.*, vol. 49, no. 3, pp. 258–268, Sep. 2003.
- [7]K. Bae, J. G. Andrews, and E. J. Powers, "Adaptive active constellation extension algorithm for peak-to-average ratio reduction in OFDM," *IEEE Commun. Lett.*, vol. 14, no. 1, pp. 39–41, Jan. 2010.
- [8]P. Van Eetvelt, G. Wade, and M. Tomlinson, "Peak to average power reduction for OFDM schemes by selective scrambling," *Elect. Lett.*, vol. 32, no. 21, pp. 1963–1964, Oct. 1996.
- [9]A. D. S. Jayalath and C. Tellambura, "Reducing the peak-to-average power ratio of orthogonal frequency division multiplexing signal through bit or symbol interleaving," *Electron. Lett.*, vol. 36, no. 13, pp. 1161–1163, Jun. 2000.
- [10]L. J. Cimini, Jr. and N. R. Sollenberger, "Peak-to-average power ratio reduction of an OFDM signal using partial transmit sequences," *IEEE Commun. Lett.*, vol. 4, no. 3, pp. 86–88, Mar. 2000.
- [11]J.-C. Chen, "Application of quantum-inspired evolutionary algorithm to reduce PAPR of an OFDM signal using partial transmit sequences technique," *IEEE Trans. Broadcast.*, vol. 56, no. 1, pp. 110–113, Mar. 2010.
- [12] T. Jiang and C. Li, "Simple alternative multi-sequences for PAPR reduction without side information in SFBC MIMO OFDM systems," *IEEE Trans. Veh. Technol.*, vol. 61, no. 7, pp. 3311–3315, Sep. 2012.
- [13] R. W. Bauml, R. F. H. Fisher, and J. B. Huber, "Reducing the peak-to-average power ratio of multicarrier modulation by selected mapping," *Elect. Lett.*, vol. 32, no. 22, pp. 2056–2057, Oct. 1996.
- [14] C.-L. Wang and Y. Ouyang, "Low-complexity selected mapping schemes for peak-to-average power ratio reduction in OFDM systems," *IEEE Trans. Signal Process.*, vol. 53, no. 12, pp. 4652–4660, Dec. 2005.
- [15] C.-P. Li, S.-H. Wang, and C.-L. Wang, "Novel low-complexity SLM schemes for PAPR reduction in OFDM systems," *IEEE Trans. Signal Process.*, vol. 58, no. 5, pp. 2916–2921, May 2010.
- [16] S.-H. Wang, J.-C. Sie, and C.-P. Li, "A low-complexity PAPR reduction scheme for OFDMA uplink systems," *IEEE Trans. Wireless Commun.*, vol. 10, no. 4, pp. 1242–1251, Apr. 2011.
- [17] W.-W. Hu, S.-H. Wang, and C.-P. Li, "Gaussian integer sequences with ideal periodic autocorrelation functions," *IEEE Trans. Signal Process.*, vol. 60, no. 11, pp. 6074–6079, Nov. 2012.
- [18] S.-H. Wang, K.-C. Lee, C.-P. Li, and H.-J. Li, "A low-complexity symbol interleaving-based PAPR reduction scheme for OFDM systems," in *Proc. IEEE International Conference on Communications (IEEE ICC 2013)*, June 2013.